**Journal of Atomic, Molecular, Condensate & Nano Physics**
Vol. 2, No. 1, pp. 1–14, 2015
ISSN 2349-2716 (online); 2349-6088 (print)
Published by RGN Publications

http://www.rgnpublications.com

# Collisional Excitation of Fluorine Like Tungsten using Relativistic Dirac Atomic R-matrix Method

Research Article

Arun Goyal[1,*], Indu Khatri[1], Sunny Aggarwal[1,3], A.K. Singh[2], Rinku Sharma[4], Man Mohan[1]

[1] *Department of Physics and Astrophysics, University of Delhi, Delhi 110007, India*
[2] *Department of Physics, D.D.U. College, University of Delhi, Delhi 110015, India*
[3] *Department of Physics, Shyamlal College, University of Delhi, Delhi 110032, India*
[4] *Department of Physics, Delhi Technological University, Delhi 110042, India*
***Corresponding author:** arun.goyal.du@gmail.com

**Abstract.** We report the new extensive calculations for collision strengths and effective collision strengths of Electron impact excitation of fine structure transitions in F-like W using fully relativistic Dirac Atomic R-matrix Code. We have included all 113 target states which belong to $2s^2 2p^5$, $2s2p^6$, $2s^2 2p^4 3l$, $2s2p^5 3l$, $2p^6 3l$ configurations. The convergence of reported collision strengths is tested by performing the same calculations for lesser number of target states which verify the individuality of our results.Effective collision strengthsover a wide temperature range $10^4$-$10^7$ K are computed. Further, to assess the accuracy and authenticity of our target states energies, a similar parallel calculation has also been performed using a fully *relativistic distorted wave* (RDW) method and a comparison of energy levels with NIST, FAC and other experimental observations has been made. We believe that the collision strength results for all forbidden transitions within the 113 fine structure levels, presented in this paper will play a substantial role in fusion plasma diagnostics.

**Keywords.** Energy levels; Collision strength; Excitation

**PACS.** 34.80.Dp

**Received:** January 22, 2015 **Accepted:** June 19, 2015

## 1. Introduction

Tungsten has moved into the focus of fusion research as it is planned to be employed as a plasma facing material in upcoming large tokomaks [1] and future fusion reactor. Due to high temperatures of fusion plasmas, atomic data, such as energy levels, radiative rates and collision strengths are required for tungsten ions to control the radiation loss. Consequently, there have been several observational and theoretical studies on tungsten ions in many charge states of tungsten. In recent years neutral and highly charged tungsten ions are included in most of the studies [2–41]. Medium charge tungsten ions have also been observed in tokomaks plasmas [42–46], but complex transitions arrays are still considered as unresolved quasi continua thus making individual ions hard to identify. These data have been compiled by NIST (National Institute of Standards and Technology) and are available at their website `http://physics.nist.gov/PhysRefData/ASD/levels`. Recently, tungsten has become a material of interest in plasma construction due to its high melting temperature, tensile strength and low hydrogen retention [42–57].

In the past, various experimental and theoretical calculations for atomic data have been done for F-like ions (including F-like W) [2, 58–60]. On the theoretical side, Cheng et al. [59] hascalculated transition wavelengths, oscillator strengths, line strengths and radiative rates for E1, E2 and M1 transition with $2s^n 2p^m$ configurations for many ions (including F-like W) using multi-configuration Dirac-Fock method.Further, Ivanova and Glushkov [60] has used the relativistic perturbation theory to calculate transitions in some levels in F-like ions (also for F-like W). Magnetic dipole transition $2s^2 2p^5 {}^2P^0_{3/2}$-$^2P^0_{1/2}$ has observed in tokamaks and due to its longer wavelength it is useful for determining ion temperature by Doppler broadening [62]. Recently, Jönsson et al. [58] has calculated level energies and transition rates for E1, E2 and M1 transitions using *Relativistic Configuration Interaction* (RCI) for $1s^2 2s^2 2p^5 {}^2P^0_{3/2}$-$^2P^0_{1/2}$ in many F-like ions (including F-like W). On the experimental side, Podpaly et al. [2] measured atomic data for $^2S_{1/2}$-$^2P^0_{3/2}$ transition in F-like W. To analyze experimental observation, collision strength data are required. There are very few calculations for collision strength in F-like W. A calculation of collision strength for F-like W using relativistic distorted-wave method for lowest three levels has been performed by Sampson et al. [61]. However, they [61] have not included contributions from resonances, which can significantly affect the effective collision strengths. Recently, Aggarwal [37] has calculated the energy levels and radiative rates for F-like W for 60 levels belonging to the configurations $2s^2 2p^5$, $2s2p^6$, $2s^2 2p^4 3l$.

Since the mechanism of collision between electron and ion has a significant contribution to study several types of plasmas and in the theoretical calculation of the line intensity ratio, which can be further utilized to determine various parameters such as densities, elemental abundances, electron temperature, etc.Therefore, the ultimate purpose of this work is to provide reliable collision strengths for plasma applications. So in the present paper, we report calculations for collision strengths for forbidden transitions for all 113 fine structure levels of $2s^2 2p^5$, $2s2p^6$, $2s^2 2p^4 3l$, $2s2p^5 3l$, $2p^6 3l$ with relativistic Dirac Atomic R-matrix method for F-like W. We have also computed the effective collision strength for 1-2 transition. We have included QED and Breit corrections to our results. QED corrections are due to vacuum polarization and self-energy effects in the first order perturbation theory and Breit correction is the correction to the Coulomb repulsion due to the exchange of virtual photon between two electrons.

## 2. Method of calculation

The relativistic effects become more significant and considerable for heavy elements and highly charged ions and hence current DARC is developed to obtain this objective. For a system of $N+1$ electrons, the Dirac Hamiltonian automatically involves Darwin term, mass-corrections term, spin-orbit term and other relativistic effects in the BPRM (Breit-Pauli R-matrix method). In the middle of 1970s, Chang founded the *Dirac R-matrix method* (DRM) theory for *electron impact excitation* (EIE) [63–65] which is an extension of the R-matrix method developed by Burke et al. [66] and BPRM method by Scott and Burke [67] and Scott and Taylor [68]. It wasagain programmed and modified in detail by Norrington [69] using the fully relativistic GRASP code derived from MCDF/BENA codes originally developed by Grant et al. [70] and revised by Norrington [69]. This code has been successfully employed to calculate atomic data for highly charged ions [71–75].

The Dirac-Coulomb Hamiltonian for electrons $i$ and $j$ can be written as

$$H^{N+1} = \sum_{i=1}^{M+1} -ic\vec{\alpha}\cdot\vec{\nabla}_i + (\beta-1)c^2 + V(r_i) + \sum_{j=i+1}^{M+1}\frac{1}{r_{ij}}. \tag{1}$$

Where $M$ is valence electrons in target, $V(r)$ is the model potential, $\alpha$, $\beta$ are $4\times4$ Dirac matrices and $c$ is speed of light. The approach of Dirac R-matrix method towards scattering includes division of configuration space into two regions, namely internal and external regions, by a spherical surface of radius $r$. For internal region, the coupled state of $(N+1)$-electron system build from target state $\Phi = |J^t M\rangle$ and scattering state $\varphi = |jm\rangle$ is defined as

$$A[\Phi,\varphi]^{J,M} = \sum C(J^t jJ; M^t mM)|J^t M^t\rangle\,|jm\rangle\,, \tag{2}$$

where $A$ is an asymmetrisation operator. On the surface of the internal region only continuum orbitals are non-zero. The single particle continuum orbitals are solutions to the differential equations (3) and (4)

$$\frac{dD_{\epsilon k,i}(r)}{dr} = -\frac{\kappa}{r}D_{\epsilon k,i}(r) + \left(2c + \frac{\epsilon}{c} - \frac{V(r)}{c}\right)\mathrm{F}_{\epsilon k,i}(r) - \sum_{i=1}^{n}\frac{\lambda_{il}Q_{nl}}{c}, \tag{3}$$

$$\frac{dF_{\epsilon k,i}(r)}{dr} = \frac{\kappa}{r}F_{\epsilon k,i}(r) - \left(\frac{\epsilon}{c} - \frac{V(r)}{c}\right)D_{\epsilon k,i}(r) + \sum_{i=1}^{n}\frac{\lambda_{il}P_{nl}}{c}. \tag{4}$$

Where $(P,Q)$ are target functions, $\lambda_{il}$ are Lagrange multipliers and $\varepsilon$ is the channel energy. The boundary condition at $r=a$ derived by combining the differential equations (3) and (4) and using the orthogonality of the continuum functions is given as

$$\frac{D_i(a)}{F_i(a)} = \frac{b+\kappa}{2ac}. \tag{5}$$

Over the internal region an orthonormal set of wave functions is derived by diagonalising the $(N+1)$-Hamiltonian matrix $\langle\Theta_k|H^{N+1}|\Theta_k\rangle$ and it can be written as

$$\psi_k = \sum_{ij} c_{ijk}A[\Phi_i,\varphi_{ij}] + \sum_m d_{mk}\theta_m \tag{6}$$

With eigenvalue $E-k^{N+1}$ and and eigenvector $(c_{ijk}, d_{mk})$ where $k$ and $j$ are index of eigenvector, continuum basis functions for a particular $\kappa$ value respectively and $i$ is the channel index representing a pair $(J^t\pi^t, \kappa)$.

At the boundary, the large radial component of the continuum electron in terms of R-matrix can be written as

$$D_i(a) = \sum_j R_{ij}[2acF_j(a) - (b+\kappa)D_j(a)]. \tag{7}$$

Where $R_{ij}$ is defined as

$$R_{ij} = \frac{1}{2a}\sum_k \frac{\omega_{ik}(a)\omega_{jk}(a)}{E_k^{N+1} - E}. \tag{8}$$

Where $\omega$ is surface amplitude.

Szmytkowski and Hinze [76] have proved that the R-matrix expression in equation (8) hassmall errors and after the truncation of R-matrix expansion, Buttle correction [64,77] given in equation (9) is adopted by them [76] to remove the errors.

$$R_{ii}^c = \left(\frac{2acF_i^c(a) - b - \kappa}{D_i^c(a)}\right)^{-1} - \frac{1}{2a}\sum_{k=1}^{K}\frac{D_{ik}^2(a)}{\epsilon_{ik} - \epsilon_i^c}. \tag{9}$$

In the external region $(r > a)$ electron exchange and correlation of a continuum electron with the atom is negligible and scattered electron wave functions satisfies the coupled radial differential equations (10) and (11)

$$\frac{dD_{\epsilon k,i}(r)}{dr} = -\frac{\kappa}{r}D_{\epsilon k,i}(r) + \left(2c + \frac{\epsilon}{c} - \frac{V(r)}{c}\right)F_{\epsilon k,i}(r) - \sum_{j=1}^{n}\sum_{\lambda=1}^{m}\frac{a_{ij}^{\lambda} r^{-\lambda-1} Q_{\epsilon k,j}}{c} \tag{10}$$

$$\frac{dF_{\epsilon k,i}(r)}{dr} = \frac{\kappa}{r}F_{\epsilon k,i}(r) - \left(\frac{\epsilon}{c} - \frac{V(r)}{c}\right)D_{\epsilon k,i}(r) + \sum_{j=1}^{n}\sum_{\lambda=1}^{m}\frac{a_{ij}^{\lambda} r^{-\lambda-1} P_{\epsilon k,j}}{c}. \tag{11}$$

Where $V(r) = (Z-N)/r$, $m$ depends on channel index $i$ and $j$ and $a_{ij}^{\lambda}$ denotes asymptotic scattering coefficients which are given by

$$a_{ij}^{\lambda} = Ang\langle[\varphi_i, \phi_i]|\ \sum_{k=1}^{N} r_k^{\lambda} P_{\lambda}(\cos\theta_{k,N+1})\ |[\varphi_j, \phi_j]\rangle. \tag{12}$$

Where *Ang* indicating the integration of outer electron radial coordinate $r_{N+1} = r$ is left out. Expressions for $S$ and $K$ matrices can be derived by linking the internal and external wave-functions.

For our calculations on energy levels, we have used the fully relativistic MCDF method revised by Norrington [69]. It also includes higher order relativistic corrections arising from the Briet interaction and *quantum electrodynamics* (QED) effects. *Extended average level* (EAL) is used to minimize the weighted size trace of the Hamiltonian matrix and to optimize the energy levels. We have also performed another independent calculation using the *Flexible Atomic Code*

(FAC). It is fully relativistic and is based on distorted-wave method and generally provides results comparable with MCDF. For calculations of Collision strength, we have used *Dirac Atomic R-matrix code* (DARC) [69] which uses Dirac-Coulomb Hamiltonian and is based on $jj$ coupling scheme. It includes the relativistic effects in a systematic way in target description as well as in scattering process. DCOUL module of DARC is used to solve the external region equations.

## 3. Result and Discussion

### 3.1 Energy Levels

The wave functions generated from the configurations $2s^2 2p^5$, $2s2p^6$, $2s^2 2p^4 3l$, $2s2p^5 3l$, $2p^6 3l$ give rise to 113 fine structure levels. Energies relative to ground state for lowest 113 states are given in Table 1 and are used to construct the target in scattering calculations. In this Table 1, we have listed the experimental observed by Beiersdorfer et al. [78] to estimate the accuracy of wave functions used in the representation of target states. The maximum % difference of our MCDF results with experimental results is 0.379%. We have also computed the energies of 113 levels using Flexible Atomic Code (FAC) which is also fully relativistic and uses the distorted wave method [79]. Its higher efficiency and user friendly platform makes the large scale calculations possible within a short interval of time.

### 3.2 Collision Strength

Since the effect of resonances put a large impact on forbidden transitions in the threshold region. Therefore, we calculate the collision strength for forbidden transitions by electron impact excitation in the present paper within 113 states using the R-matrix method. In our calculations 24 continuum orbitals per angular momentum are used in the expansion of wave-functions. The R-matrix boundary automatically calculated by the code to include the maximum number of target functions is 0.66 a.u. The maximum number of channels for a partial wave is 509 and the corresponding size of the Hamiltonian matrix is 12266. In order to obtain the convergence in collision strength $\Omega$ all partial waves corresponding to $2J \leq 18$ are included.

Collision strength ($\Omega$) and collision cross-section ($\sigma_{ij}$) are connected by the following expression

$$\Omega_{ij} = k_i^2 \omega_i \sigma_{ij}(E). \tag{13}$$

Where $k_i^2$ is the incident energy of the electron, $\omega_i$ is statistical weight of the initial state. $\Omega$ is adimensionless and symmetric quantity. For brevity, we have listed collision strengths at four incident energies of electron from 1000 Ryd. to 1600 Ryd. at an interval of 200 Ryd bergs from the ground state in Table 2. We have listed collision strengths for all other forbidden transitions in Table 3. The indices for lower level $i$ and upper level $j$ of a transition in Table 2 are specified in the first column of Table 1. In Table 2, we have also tabulated collision strengths for the lowest 52 levels and the convergence of results is examined. To highlight the contribution of resonances in the resonance region, the value of collision strength is shown in Figure 1(a) for forbidden transitions 1-2. The resonances at energies in the threshold region are physically meaningful. From Figure 1, it can be clearly seen that resonances dominate the collision strength and

their magnitude are very large.Due to the inclusion of pseudo orbitals in the wave function expansion, pseudo-resonances appear at higher energies [80]. Hence, proper averaging over pseudo-resonances are essential to neutralize the distortion of the most accurate results in the calculation of the effective collision strengths. Sampson et al. [61] have presented their solutions in terms of scattered electron energies instead of incident electron energies, so there is no common data between two sets of results for comparison. Therefore, our reported collision may be taken as benchmark in future and can be used for the calculation of effective collision strengths and rate coefficients for forbidden transitions.

**Table 1.** MCDF Dirac-Coulomb (DC), Breit and quantum electrodynamics (QED) contribution to energies (in Ryd.) and comparison with FAC, NIST and ref. [77]

| Level number | Configurations | Energies (in Ryd.) | | | | | | |
|---|---|---|---|---|---|---|---|---|
| | | MCDF | | | | FAC | NIST [81] | Ref. [78] |
| | | DC | Breit | QED | Total | | | |
| 1 | $2s^22p^5\ ^2P^o_{3/2}$ | 0.00 | — | — | 0.00 | 0.00 | 0.00 | |
| 2 | $2s^22p^5\ ^2P^o_{1/2}$ | 103.22 | -1.30 | 0.12 | 102.04 | 102.16 | 102.08 | |
| 3 | $2s2p^6\ ^2S_{1/2}$ | 138.90 | -0.04 | -1.16 | 137.70 | 137.43 | 137.18 | |
| 4 | $2s^22p^4(^3_2P)3s\ ^4P_{5/2}$ | 622.14 | -1.30 | 0.17 | 621.02 | 621.06 | | 621.72 |
| 5 | $2s^22p^4(^3_2P)3s\ ^2P_{3/2}$ | 622.91 | -1.26 | 0.17 | 621.83 | 621.89 | | 622.50 |
| 6 | $2s^22p^4(^1_0S)3s\ ^2S_{1/2}$ | 626.27 | -0.64 | 0.17 | 625.80 | 625.82 | | 626.45 |
| 7 | $2s^22p^4(^3_2P)3p\ ^4P^o_{3/2}$ | 632.16 | -0.81 | -0.17 | 631.18 | 631.12 | | 631.82 |
| 8 | $2s^22p^4(^3_2P)3p\ ^2D^o_{5/2}$ | 632.50 | -1.01 | -0.17 | 631.33 | 631.27 | | 631.82 |
| 9 | $2s^22p^4(^1_0S)3p\ ^2P^o_{1/2}$ | 636.17 | -0.28 | -0.17 | 635.71 | 635.62 | | |
| 10 | $2s^22p^4(^3_2P)3p\ ^4P^o_{5/2}$ | 661.32 | -1.37 | -0.14 | 659.82 | 659.77 | | |
| 11 | $2s^22p^4(^3_2P)3p\ ^2S^o_{1/2}$ | 661.34 | -1.32 | -0.14 | 659.89 | 659.77 | | |
| 12 | $2s^22p^4(^3_2P)3p\ ^4D^o_{7/2}$ | 661.35 | -1.40 | -0.13 | 659.82 | 659.85 | | |
| 13 | $2s^22p^4(^3_2P)3p\ 4S^o_{3/2}$ | 664.63 | -1.01 | -0.14 | 663.48 | 663.42 | | |
| 14 | $2s^22p^4(^3_2P)3p\ ^2P^o_{3/2}$ | 666.29 | -0.78 | -0.14 | 665.37 | 665.29 | | |
| 15 | $2s^22p^4(^3_2P)3d\ ^4P_{3/2}$ | 671.95 | -1.11 | -0.18 | 670.65 | 670.52 | | |
| 16 | $2s^22p^4(^3_2P)3d\ ^4D_{5/2}$ | 672.40 | -1.39 | -0.18 | 670.83 | 670.69 | | |
| 17 | $2s^22p^4(^3_2P)3d\ ^4P_{1/2}$ | 672.53 | -1.25 | -0.18 | 671.10 | 670.75 | | |
| 18 | $2s^22p^4(^3_2P)3d\ ^2F_{7/2}$ | 672.60 | -1.53 | -0.18 | 670.89 | 670.97 | | |
| 19 | $2s^22p^4(^1_0S)3d\ ^2D_{3/2}$ | 676.27 | -0.75 | -0.18 | 675.34 | 675.18 | | |
| 20 | $2s^22p^4(^3_2P)3d\ ^4D_{7/2}$ | 679.10 | -1.60 | -0.18 | 677.32 | 677.19 | | |
| 21 | $2s^22p^4(^3_2P)3d\ ^4F_{9/2}$ | 679.22 | -1.68 | -0.18 | 677.36 | 677.24 | | |
| 22 | $2s^22p^4(^3_2P)3d\ ^2P_{1/2}$ | 680.07 | -1.48 | -0.18 | 678.41 | 678.28 | | |
| 23 | $2s^22p^4(^3_2P)3d\ ^2D_{5/2}$ | 681.91 | -1.51 | -0.18 | 680.22 | 680.08 | | 680.61 |
| 24 | $2s^22p^4(^1_2D)3d\ ^2P_{3/2}$ | 682.00 | -1.50 | -0.18 | 680.32 | 680.18 | | 680.61 |
| 25 | $2s^22p^4(^1_0S)3d\ ^2D_{5/2}$ | 684.11 | -1.02 | -0.18 | 682.91 | 682.75 | | 683.20 |
| 26 | $2s^22p^4(^3_2P)3s\ ^4P_{3/2}$ | 725.62 | -2.32 | 0.29 | 723.59 | 723.71 | | |
| 27 | $2s^22p^4(^3_2P)3s\ ^2P_{1/2}$ | 726.34 | -2.32 | 0.29 | 724.31 | 724.44 | | |
| 28 | $2s^22p^4(^1_2D)3s\ ^2D_{5/2}$ | 727.73 | -2.93 | 0.29 | 725.09 | 725.20 | | |

*Table Contd.*

| Level number | Configurations | Energies (in Ryd.) | | | | | | |
|---|---|---|---|---|---|---|---|---|
| | | MCDF | | | | FAC | NIST [81] | Ref. [78] |
| | | DC | Breit | QED | Total | | | |
| 29 | $2s^22p^4(^1_2D)3s\ ^2D_{3/2}$ | 728.10 | -2.84 | 0.29 | 725.55 | 725.67 | | |
| 30 | $2s^22p^4(^3_2P)3p\ ^4P^o_{1/2}$ | 735.39 | -1.95 | -0.05 | 733.39 | 733.39 | | |
| 31 | $2s^22p^4(^3_2P)3p\ ^4D^o_{3/2}$ | 736.08 | -2.16 | -0.05 | 733.87 | 733.87 | | |
| 32 | $2s^22p^4(^1_2D)3p\ ^2F^o_{5/2}$ | 737.63 | -2.68 | -0.05 | 734.90 | 734.90 | | |
| 33 | $2s^22p^4(^1_2D)3p\ ^2P^o_{3/2}$ | 740.37 | -2.23 | -0.05 | 738.09 | 738.06 | | |
| 34 | $2s2p^5(^2_1P)3s\ ^4P^o_{5/2}$ | 756.45 | -1.52 | -0.95 | 753.98 | 753.79 | | |
| 35 | $2s2p^5(^2_1P)3s\ ^2P^o_{3/2}$ | 758.47 | -1.42 | -0.96 | 756.09 | 755.89 | | |
| 36 | $2s2p^5(^2_1P)3s\ ^2P^o_{1/2}$ | 762.75 | -1.60 | -0.81 | 760.35 | 760.28 | | |
| 37 | $2s2p^5(^2_1P)3s\ ^2P^o_{3/2}$ | 763.61 | -1.40 | -0.88 | 761.32 | 761.19 | | |
| 38 | $2s^22p^4(^3_2P)3p\ ^4D^o_{5/2}$ | 764.87 | -2.35 | -0.04 | 762.48 | 762.50 | | |
| 39 | $2s^22p^4(^3_2P)3p\ ^2D^o_{3/2}$ | 765.34 | -2.45 | -0.05 | 762.84 | 762.88 | | |
| 40 | $2s^22p^4(^3_2P)3p\ ^2P^o_{1/2}$ | 765.65 | -2.16 | -0.17 | 763.32 | 763.21 | | |
| 41 | $2s^22p^4(^1_2D)3p\ ^2F^o_{7/2}$ | 766.70 | -3.06 | -0.02 | 763.63 | 763.65 | | |
| 42 | $2s2p^5(^2_1P)3p\ 4S_{3/2}$ | 767.00 | -0.98 | -1.32 | 764.69 | 764.40 | | |
| 43 | $2s^22p^4(^1_2D)3p\ ^2D^o_{3/2}$ | 767.21 | -2.52 | -0.11 | 764.58 | 764.47 | | |
| 44 | $2s2p^5(^2_1P)3p\ ^2D_{5/2}$ | 767.33 | -1.26 | -1.31 | 764.75 | 764.51 | | |
| 45 | $2s^22p^4(^1_2D)3p\ ^2D^o_{5/2}$ | 767.47 | -2.86 | -0.02 | 764.59 | 764.62 | | |
| 46 | $2s^22p^4(^1_2D)3p\ ^2P^o_{1/2}$ | 771.29 | -2.50 | -0.04 | 768.75 | 768.75 | | |
| 47 | $2s2p^5(^2_1P)3p\ ^2P_{1/2}$ | 773.04 | -0.99 | -1.29 | 770.76 | 770.48 | | |
| 48 | $2s2p^5(^2_1P)3p\ ^2D_{3/2}$ | 773.27 | -1.01 | -1.30 | 770.96 | 770.66 | | |
| 49 | $2s^22p^4(^3_2P)3d\ ^4D_{1/2}$ | 775.03 | -2.28 | -0.06 | 772.68 | 772.63 | | |
| 50 | $2s^22p^4(^3_2P)3d\ ^4D_{3/2}$ | 776.07 | -2.45 | -0.07 | 773.55 | 773.50 | | |
| 51 | $2s^22p^4(^3_2P)3d\ ^4F_{5/2}$ | 776.62 | -2.57 | -0.07 | 773.98 | 773.93 | | |
| 52 | $2s^22p^4(^1_2D)3d\ 2G_{7/2}$ | 777.72 | -3.16 | -0.06 | 774.50 | 774.44 | | |
| 53 | $2s^22p^4(^1_2D)3d\ ^2S_{1/2}$ | 778.99 | -2.78 | -0.10 | 776.11 | 776.00 | | 776.63 |
| 54 | $2s^22p^4(^1_2D)3d\ ^2F_{5/2}$ | 779.26 | -3.01 | -0.07 | 776.18 | 776.10 | | 776.63 |
| 55 | $2s^22p^4(^1_2D)3d\ ^2D_{3/2}$ | 779.53 | -2.86 | -0.08 | 776.59 | 776.49 | | 776.63 |
| 56 | $2s^22p^4(^3_2P)3d\ ^4F_{7/2}$ | 782.49 | -2.68 | -0.07 | 779.74 | 779.69 | | |
| 57 | $2s^22p^4(^3_2P)3d\ ^4P_{5/2}$ | 783.39 | -2.57 | -0.06 | 780.76 | 780.72 | | |
| 58 | $2s^22p^4(^3_2P)3d\ ^2P_{3/2}$ | 783.61 | -2.72 | -0.06 | 780.82 | 780.78 | | |
| 59 | $2s^22p^4(^1_2D)3d\ 2G_{9/2}$ | 784.60 | -3.29 | -0.06 | 781.25 | 781.19 | | |
| 60 | $2s^22p^4(^1_2D)3d\ ^2D_{5/2}$ | 785.05 | -3.07 | -0.07 | 781.91 | 781.86 | | |
| 61 | $2s^22p^4(^1_2D)3d\ ^2F_{7/2}$ | 785.57 | -3.11 | -0.06 | 782.39 | 782.34 | | |
| 62 | $2s^22p^4(^3_2P)3d\ ^2D_{3/2}$ | 787.19 | -3.02 | -0.06 | 784.11 | 784.03 | | |
| 63 | $2s^22p^4(^1_2D)3d\ ^2P_{1/2}$ | 787.80 | -3.17 | -0.07 | 784.56 | 784.48 | | |
| 64 | $2s2p^5(^2_1P)3p\ ^4D_{7/2}$ | 795.95 | -1.57 | -1.28 | 793.10 | 792.82 | | |
| 65 | $2s2p^5(^2_1P)3p\ ^2P_{3/2}$ | 796.45 | -1.50 | -1.29 | 793.67 | 793.40 | | |
| 66 | $2s2p^5(^2_1P)3p\ ^4P_{5/2}$ | 796.88 | -1.44 | -1.28 | 794.15 | 793.88 | | |
| 67 | $2s2p^5(^2_1P)3p\ ^2S_{1/2}$ | 798.47 | -1.41 | -1.29 | 795.77 | 795.46 | | |
| 68 | $2s2p^5(^2_1P)3p\ ^2D_{5/2}$ | 802.35 | -1.33 | -1.29 | 799.73 | 799.42 | | |
| 69 | $2s2p^5(^2_1P)3p\ ^2P_{3/2}$ | 802.75 | -1.23 | -1.29 | 800.23 | 799.93 | | |
| 70 | $2s2p^5(^2_1P)3p\ ^2S_{1/2}$ | 804.95 | -1.13 | -1.29 | 802.54 | 802.18 | | |

*Table Contd.*

| Level number | Configurations | Energies (in Ryd.) | | | | | | |
|---|---|---|---|---|---|---|---|---|
| | | MCDF | | | | FAC | NIST [81] | Ref. [78] |
| | | DC | Breit | QED | Total | | | |
| 71 | $2s2p^5(^2_1P)3d\ ^4P^o_{1/2}$ | 806.00 | -1.23 | -1.34 | 803.44 | 803.07 | | |
| 72 | $2s2p^5(^2_1P)3d\ ^4P^o_{3/2}$ | 806.89 | -1.41 | -1.34 | 804.14 | 803.77 | | |
| 73 | $2s2p^5(^2_1P)3d\ ^2F^o_{7/2}$ | 807.43 | -1.73 | -1.34 | 804.36 | 803.98 | | |
| 74 | $2s2p^5(^2_1P)3d\ ^4D^o_{5/2}$ | 807.48 | -1.47 | -1.34 | 804.67 | 804.28 | | |
| 75 | $2s2p^5(^2_1P)3d\ ^2P^o_{1/2}$ | 813.01 | -1.22 | -1.34 | 810.45 | 809.82 | | |
| 76 | $2s2p^5(^2_1P)3d\ ^2F^o_{5/2}$ | 813.12 | -1.43 | -1.34 | 810.36 | 809.94 | | |
| 77 | $2s2p^5(^2_1P)3d\ ^2D^o_{3/2}$ | 813.27 | -1.29 | -1.34 | 810.64 | 810.03 | | |
| 78 | $2s2p^5(^2_1P)3d4F^o_{9/2}$ | 813.40 | -1.87 | -1.34 | 810.19 | 810.23 | | |
| 79 | $2s2p^5(^2_1P)3d\ ^4D^o_{7/2}$ | 814.78 | -1.70 | -1.34 | 811.74 | 811.37 | | |
| 80 | $2s2p^5(^2_1P)3d\ ^2D^o_{5/2}$ | 814.80 | -1.62 | -1.34 | 811.84 | 811.47 | | |
| 81 | $2s2p^5(^2_1P)3d\ ^2P^o_{3/2}$ | 816.20 | -1.59 | -1.34 | 813.27 | 812.89 | | |
| 82 | $2s2p^5(^2_1P)3d\ ^2P^o_{1/2}$ | 817.77 | -1.68 | -1.34 | 814.76 | 814.35 | | |
| 83 | $2s2p^5(^2_1P)3d\ ^2F^o_{7/2}$ | 820.29 | -1.56 | -1.34 | 817.39 | 816.98 | | |
| 84 | $2s2p^5(^2_1P)3d\ ^2D^o_{5/2}$ | 820.76 | -1.45 | -1.34 | 817.97 | 817.57 | | |
| 85 | $2s2p^5(^2_1P)3d\ ^2P^o_{3/2}$ | 821.93 | -1.57 | -1.34 | 819.02 | 818.58 | | |
| 86 | $2s^22p^4(^3_2P)3s\ ^4P_{1/2}$ | 832.81 | -3.53 | 0.40 | 829.68 | 829.88 | | |
| 87 | $2s^22p^4(^3_2P)3p\ ^4D^o_{1/2}$ | 843.94 | -3.22 | 0.05 | 840.76 | 840.84 | | |
| 88 | $2s2p^5(^2_1P)3s\ ^4P^o_{1/2}$ | 861.65 | -2.47 | -0.86 | 858.32 | 858.19 | | |
| 89 | $2s2p^5(^2_1P)3s\ ^4P^o_{3/2}$ | 864.34 | -2.86 | -0.84 | 860.65 | 860.52 | | |
| 90 | $2s2p^5(^2_1P)3s\ ^2P^o_{1/2}$ | 866.40 | -2.65 | -0.87 | 862.88 | 862.74 | | |
| 91 | $2s2p^5(^2_1P)3p\ ^4D_{1/2}$ | 871.68 | -2.19 | -1.21 | 868.29 | 868.06 | | |
| 92 | $2s^22p^4(^1_0S)3p\ ^2P^o_{3/2}$ | 872.05 | -3.53 | 0.06 | 868.59 | 868.70 | | |
| 93 | $2s2p^5(^2_1P)3p\ ^4D_{3/2}$ | 874.51 | -2.62 | -1.20 | 870.70 | 870.46 | | |
| 94 | $2s2p^5(^2_1P)3p\ ^4P_{1/2}$ | 877.56 | -2.25 | -1.20 | 874.10 | 870.58 | | |
| 95 | $2s^22p^4(^3_2P)3d\ ^4F_{3/2}$ | 884.07 | -3.74 | 0.04 | 880.36 | 870.85 | | |
| 96 | $2s^22p^4(^3_2P)3d\ ^2F_{5/2}$ | 889.96 | -3.78 | 0.04 | 886.22 | 873.81 | | |
| 97 | $2p^63s\ ^2S_{1/2}$ | 900.31 | -1.71 | -1.88 | 896.71 | 874.73 | | |
| 98 | $2s2p^5(^2_1P)3p\ ^4P_{3/2}$ | 900.62 | -2.49 | -1.17 | 896.96 | 874.77 | | |
| 99 | $2s2p^5(^2_1P)3p\ ^4D_{5/2}$ | 903.79 | -2.88 | -1.17 | 899.74 | 875.11 | | |
| 100 | $2s2p^5(^2_1P)3p\ ^2D_{3/2}$ | 903.97 | -2.80 | -1.17 | 899.99 | 879.18 | | |
| 101 | $2s2p^5(^2_1P)3p\ ^2P_{1/2}$ | 905.23 | -2.25 | -1.41 | 901.57 | 880.38 | | |
| 102 | $2p^63p\ ^2P^o_{1/2}$ | 910.68 | -1.20 | -2.39 | 907.08 | 886.25 | | |
| 103 | $2s2p^5(^2_1P)3d\ ^4F^o_{3/2}$ | 911.80 | -2.59 | -1.22 | 907.99 | 886.53 | | |
| 104 | $2s2p^5(^2_1P)3d\ ^4F^o_{5/2}$ | 914.82 | -2.99 | -1.22 | 910.61 | 886.54 | | |
| 105 | $2s2p^5(^2_1P)3d\ ^4D^o_{3/2}$ | 916.05 | -2.98 | -1.22 | 911.85 | 886.58 | | |
| 106 | $2s2p^5(^2_1P)3d\ ^4D^o_{1/2}$ | 916.56 | -2.66 | -1.29 | 912.61 | 887.85 | | |
| 107 | $2s2p^5(^2_1P)3d\ ^4P^o_{5/2}$ | 918.63 | -2.74 | -1.22 | 914.67 | 890.66 | | |
| 108 | $2s2p^5(^2_1P)3d\ ^4F^o_{7/2}$ | 921.59 | -3.12 | -1.22 | 917.25 | 890.70 | | |
| 109 | $2s2p^5(^2_1P)3d\ ^2F^o_{5/2}$ | 922.20 | -3.00 | -1.22 | 917.98 | 890.70 | | |
| 110 | $2s2p^5(^2_1P)3d\ ^2D^o_{3/2}$ | 922.26 | -2.94 | -1.22 | 918.10 | 890.78 | | |
| 111 | $2p^63p\ ^2P^o_{3/2}$ | 940.15 | -1.28 | -2.42 | 936.44 | 891.24 | | |
| 112 | $2p^63d\ ^2D_{3/2}$ | 951.00 | -1.34 | -2.48 | 947.18 | 893.51 | | |
| 113 | $2p^63d\ ^2D_{5/2}$ | 957.98 | -1.49 | -2.48 | 954.01 | 893.53 | | |

**Table 2.** Fine structure collision Strengths of forbidden transitions from ground state for 52 levels and 113 levels for W LXVI

| Transition | | Collision Strength | | | | | | | |
|---|---|---|---|---|---|---|---|---|---|
| | | 52 levels | 113 levels | 52 levels | 113 levels | 52 levels | 113 levels | 52 levels | 113 levels |
| *i* | *j* | 1000 Ryd. | 1000 Ryd. | 1200 Ryd. | 1200 Ryd. | 1400 Ryd. | 1400 Ryd. | 1600 Ryd. | 1600 Ryd. |
| 1 | 2 | 2.116E-03 | 2.110E-03 | 2.017E-03 | 2.010E-03 | 1.912E-03 | 1.910E-03 | 1.858E-03 | 1.860E-03 |
| 1 | 7 | 4.539E-04 | 4.540E-04 | 3.967E-04 | 3.970E-04 | 3.411E-04 | 3.410E-04 | 3.009E-04 | 3.010E-04 |
| 1 | 8 | 9.372E-04 | 9.360E-04 | 8.838E-04 | 8.820E-04 | 8.160E-04 | 8.140E-04 | 7.569E-04 | 7.550E-04 |
| 1 | 9 | 2.821E-04 | 2.820E-04 | 2.603E-04 | 2.600E-04 | 2.357E-04 | 2.350E-04 | 2.161E-04 | 2.160E-04 |
| 1 | 10 | 5.977E-04 | 6.010E-04 | 5.119E-04 | 5.150E-04 | 4.312E-04 | 4.340E-04 | 3.750E-04 | 3.770E-04 |
| 1 | 11 | 2.171E-04 | 2.180E-04 | 1.847E-04 | 1.860E-04 | 1.547E-04 | 1.560E-04 | 1.336E-04 | 1.350E-04 |
| 1 | 12 | 6.767E-04 | 6.800E-04 | 5.703E-04 | 5.730E-04 | 4.720E-04 | 4.740E-04 | 4.057E-04 | 4.080E-04 |
| 1 | 13 | 4.473E-03 | 4.480E-03 | 4.651E-03 | 4.660E-03 | 4.703E-04 | 4.710E-03 | 4.801E-03 | 4.810E-03 |
| 1 | 14 | 7.576E-03 | 7.580E-03 | 7.878E-03 | 7.880E-03 | 7.970E-03 | 7.970E-03 | 8.159E-03 | 8.160E-03 |
| 1 | 30 | 9.374E-05 | 9.350E-05 | 7.701E-05 | 7.690E-05 | 6.110E-05 | 6.090E-05 | 5.265E-05 | 5.250E-05 |
| 1 | 31 | 4.684E-04 | 4.700E-04 | 4.492E-04 | 4.510E-04 | 4.214E-04 | 4.230E-04 | 4.172E-04 | 4.190E-04 |
| 1 | 32 | 2.856E-04 | 2.840E-04 | 2.346E-04 | 2.340E-04 | 1.861E-04 | 1.850E-04 | 1.604E-04 | 1.600E-04 |
| 1 | 33 | 6.987E-03 | 6.910E-03 | 7.304E-03 | 7.230E-03 | 7.374E-03 | 7.300E-03 | 7.668E-03 | 7.590E-03 |
| 1 | 34 | 2.742E-04 | 2.700E-04 | 2.211E-04 | 2.180E-04 | 1.768E-04 | 1.750E-04 | 1.500E-04 | 1.490E-04 |
| 1 | 35 | 3.332E-03 | 3.320E-03 | 3.489E-03 | 3.480E-03 | 3.550E-03 | 3.540E-03 | 3.695E-03 | 3.680E-03 |
| 1 | 36 | 1.155E-04 | 1.140E-04 | 9.386E-05 | 9.280E-05 | 7.551E-05 | 7.480E-05 | 6.457E-05 | 6.400E-05 |
| 1 | 37 | 4.611E-03 | 4.600E-03 | 4.842E-03 | 4.830E-03 | 4.939E-03 | 4.930E-03 | 5.149E-03 | 5.140E-03 |
| 1 | 38 | 2.775E-04 | 2.780E-04 | 2.367E-04 | 2.380E-04 | 1.989E-04 | 1.990E-04 | 1.773E-04 | 1.780E-04 |
| 1 | 39 | 2.643E-04 | 2.650E-04 | 2.518E-04 | 2.530E-04 | 2.365E-04 | 2.380E-04 | 2.297E-04 | 2.310E-04 |
| 1 | 40 | 7.187E-05 | 7.210E-05 | 6.365E-05 | 6.400E-05 | 5.568E-05 | 5.590E-05 | 5.104E-05 | 5.130E-05 |
| 1 | 41 | 3.876E-04 | 3.860E-04 | 3.464E-04 | 3.460E-04 | 3.048E-04 | 3.040E-04 | 2.777E-04 | 2.770E-04 |
| 1 | 43 | 2.728E-04 | 2.730E-04 | 2.523E-04 | 2.520E-04 | 2.309E-04 | 2.310E-04 | 2.232E-04 | 2.230E-04 |
| 1 | 45 | 2.907E-04 | 2.910E-04 | 2.556E-04 | 2.560E-04 | 2.219E-04 | 2.220E-04 | 2.021E-04 | 2.020E-04 |
| 1 | 46 | 9.592E-05 | 9.610E-05 | 8.253E-05 | 8.270E-05 | 7.011E-05 | 7.020E-05 | 6.303E-05 | 6.310E-05 |
| 1 | 71 | | 1.010E-04 | | 8.320E-05 | | 6.970E-05 | | 5.990E-05 |
| 1 | 72 | | 2.500E-04 | | 2.220E-04 | | 2.010E-04 | | 1.850E-04 |
| 1 | 73 | | 1.200E-03 | | 1.240E-03 | | 1.260E-03 | | 1.260E-03 |
| 1 | 74 | | 5.630E-04 | | 5.530E-04 | | 5.450E-04 | | 5.360E-04 |
| 1 | 75 | | 4.040E-04 | | 4.380E-04 | | 4.620E-04 | | 4.760E-04 |
| 1 | 76 | | 3.690E-04 | | 3.260E-04 | | 2.950E-04 | | 2.720E-04 |
| 1 | 77 | | 2.610E-04 | | 2.350E-04 | | 2.160E-04 | | 2.020E-04 |
| 1 | 79 | | 1.020E-03 | | 1.030E-03 | | 1.040E-03 | | 1.040E-03 |
| 1 | 80 | | 1.240E-03 | | 1.340E-03 | | 1.420E-03 | | 1.470E-03 |
| 1 | 81 | | 1.330E-03 | | 1.490E-03 | | 1.610E-03 | | 1.680E-03 |
| 1 | 82 | | 4.180E-04 | | 4.560E-04 | | 4.850E-04 | | 5.030E-04 |
| 1 | 83 | | 1.410E-03 | | 1.490E-03 | | 1.530E-03 | | 1.550E-03 |
| 1 | 84 | | 8.640E-04 | | 9.090E-04 | | 9.440E-04 | | 9.620E-04 |
| 1 | 85 | | 1.810E-04 | | 1.420E-04 | | 1.150E-04 | | 9.490E-05 |
| 1 | 87 | | 3.620E-07 | | 2.910E-07 | | 2.370E-07 | | 2.050E-07 |
| 1 | 88 | | 1.410E-07 | | 1.250E-07 | | 1.120E-07 | | 1.030E-07 |

*Table Contd.*

| Transition | | Collision Strength | | | | | | | |
|---|---|---|---|---|---|---|---|---|---|
| | | 52 levels | 113 levels | 52 levels | 113 levels | 52 levels | 113 levels | 52 levels | 113 levels |
| $i$ | $j$ | 1000 Ryd. | 1000 Ryd. | 1200 Ryd. | 1200 Ryd. | 1400 Ryd. | 1400 Ryd. | 1600 Ryd. | 1600 Ryd. |
| 1 | 89 | | 1.390E-06 | | 1.410E-06 | | 1.420E-06 | | 1.450E-06 |
| 1 | 90 | | 4.920E-07 | | 4.330E-07 | | 3.860E-07 | | 3.590E-07 |
| 1 | 92 | | 8.370E-08 | | 6.700E-08 | | 5.450E-08 | | 4.660E-08 |
| 1 | 102 | | 3.810E-07 | | 3.560E-07 | | 3.390E-07 | | 3.290E-07 |
| 1 | 103 | | 2.970E-07 | | 2.660E-07 | | 2.500E-07 | | 2.390E-07 |
| 1 | 104 | | 9.770E-07 | | 9.270E-07 | | 8.960E-07 | | 8.750E-07 |
| 1 | 105 | | 1.590E-06 | | 1.520E-06 | | 1.470E-06 | | 1.440E-06 |
| 1 | 106 | | 9.370E-07 | | 8.750E-07 | | 8.340E-07 | | 8.030E-07 |
| 1 | 107 | | 1.420E-07 | | 1.190E-07 | | 1.050E-07 | | 9.570E-08 |
| 1 | 108 | | 1.640E-06 | | 1.670E-06 | | 1.700E-06 | | 1.700E-06 |
| 1 | 109 | | 1.130E-06 | | 1.110E-06 | | 1.110E-06 | | 1.110E-06 |
| 1 | 110 | | 3.570E-07 | | 2.940E-07 | | 2.500E-07 | | 2.190E-07 |
| 1 | 111 | | 3.610E-07 | | 3.210E-07 | | 2.850E-07 | | 2.640E-07 |

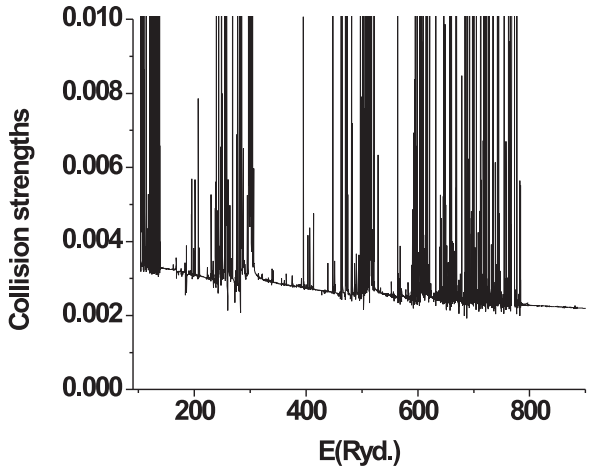


**Figure 1.** The Ω in the resonance region for transition 1-2 as a function of incident energy of electron

## 3.3 Effective Collision strength

In the present paper we have plotted the effective collision strengths as a function of temperature. The effective collision strength ($\gamma$) is defined by

$$\gamma_{i\to f} = \frac{1}{\kappa T}\int_0^\infty \exp\left(\frac{-E_f}{\kappa T}\right)\Omega_{i\to f}(E_f)d\,. \tag{14}$$

Where $\kappa$ refers to Boltzmann's constant, $T$ to absolute temperature and $E_f$ to the final energy of the scattered electron. The subscript $i$ and $f$ denote the initial and final states of atom. $E_f$ denotes the energy of incident electron with respect to upper level $f$. The effective collision strengths are calculated by integrating collision strengths over a Maxwellian distribution of electron energies for fine structure levels from threshold to infinity for lowest 113 levels.

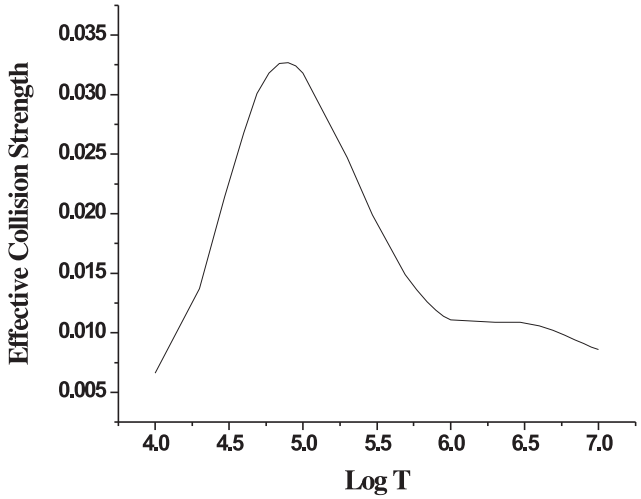


**Figure 2.** Effective Collision Strengths for 1-2 transition of W LXVI

We have presented the effective collision strengths in Table 3 for 1-2 transition over a temperature range of $10^4$-$10^7$ K applicable to the modelling of fusion plasmas and can easily be incorporated into the calculation of plasma properties.In effective collision strength plot for 1-2 transition shown in Figure 2, it can be clearly seen that the height of low lying resonances raise the effective collision strength at low temperatures.

**Table 3.** Effective collision strengths for $^2P^0_{3/2}$-$^2P^0_{1/2}$ transition in W LXVI as a function of electron temperature

| Electron temperature ($10^5$K) | Effective collision strength | Electron temperature ($10^5$K) | Effective collision strength |
|---|---|---|---|
| 0.1 | 0.0066 | 7.0 | 0.0126 |
| 0.2 | 0.0137 | 8.0 | 0.0119 |
| 0.3 | 0.0214 | 9.0 | 0.0114 |
| 0.4 | 0.0268 | 10.0 | 0.0111 |
| 0.5 | 0.0301 | 20.0 | 0.0109 |
| 0.6 | 0.0318 | 30.0 | 0.0109 |
| 0.7 | 0.0326 | 40.0 | 0.0106 |
| 0.8 | 0.0327 | 50.0 | 0.0102 |
| 0.9 | 0.0324 | 60.0 | 0.0098 |
| 1.0 | 0.0318 | 70.0 | 0.0094 |
| 2.0 | 0.0247 | 80.0 | 0.0091 |
| 3.0 | 0.0199 | 90.0 | 0.0088 |
| 5.0 | 0.0149 | 100.0 | 0.0086 |
| 6.0 | 0.0136 | | |

## 4. Conclusion

In this paper, we have generated the target wave functions from the configurations $2s^22p^5$, $2s2p^6$, $2s^22p^43l$, $2s2p^53l$, $2p^63l$ using MCDF method and presented data of excitation energies

for all fine structure levels. Our calculated energies for 113 target states calculated by using MCDF and FAC are in full agreement with energies provided by Beiersdorfer et al. [78]. We have provided collision strength data and effective collision strengths for 1-2 transition and to the best of our cognition, there is no information on collision strengths and effective collision strength of W LXVI is published anywhere in the literature and hence we provide a fresh set of data in this study.

For the subject of different type of plasmas and measurement of diverse parameters, there is a big need of collision strength data. Therefore, we affirm that the comprehensive theoretical study of our presented results for collision and effective collision strengths in the present paper will be beneficial for plasma modelling in fusion reactors and other plasma physics applications in future.

## Acknowledgement

Arun Goyal and Indu Khatri are thankful to U.G.C India for Fellowship. Authors are grateful to Anil Pradhan and Sultana N. Nahar for their guidance.

### Competing Interests

The authors declare that they have no competing interests.

### Authors' Contributions

All the authors contributed equally and significantly in writing this article. All the authors read and approved the final manuscript.

## References

[1] R. Aymar, P. Barabaschi and Y. Shimomura, Plasma Phys. Control Fusion **44** 519 (2002).

[2] Y.A. Podpaly, J. Clementson, P. Beiersdorfer, J. Williamson, G.V. Brown and M.F. Gu, *Phys. Rev. A* **80** 052504 (2009).

[3] P. Beiersdorfer, J.K. Lepson, M.B. Schneider and M.P. Bode, *Phys. Rev. A* **86** 012509 (2013).

[4] Y. Ralchenko, I.N. Draganic, J.N. Tan, J.D. Gillaspy, J.M. Pomeroy, J. Reader, U. Feldman and G.E. Holland, *J. Phys. B* **41** 021003 (2008).

[5] J. Clementson and P. Beiersdorfer, *Phys. Rev. A* **81** 052509 (2010).

[6] J. Clementson, P. Beiersdorfer, G.V. Brown and M.F. Gu, Phys. Scr. **81** 015301 (2010).

[7] G.C. Osborne, A.S. Safronova, V.L. Kantsyrev, U.I. Safronova, P. Beiersdorfer, K. Williamson, M.E. Weller and I. Shrestha, *Can. J. Phys.* **89** 599 (2011).

[8] Y. Ralchenko, I.N. Draganic, D. Osin, J.D. Gillaspy and J. Reader, *Phys. Rev. A* **83** 032517 (2011).

[9] C.F. Fischer and G. Gaigalas, *Phys. Rev. A* **85** 042501 (2012).

[10] C. Harte et al., *J. Phys. B* **43** 205004 (2010).

[11] S. Wu and R. Hutton, *Can. J. Phys.* **86** 125 (2008).

[12] J. Clementson, P. Beiersdorfer, W.E. Magee, H.S. Mclean and R.D. Wood, *J. Physics. B* **43** 144009 (2010).

[13] R. Hutton et al., Nuclear Instruments and methods in Physics Research **205** 114 (2003).

[14] T. Pütterich et al., *J. Phys. B* **38** 3071 (2005).

[15] R. Radtke et al., *Journal of Physics: Conference Series* **58** 113 (2007).

[16] R. Radtke et al., *Phys. Rev. A* **64** 012720 (2001).

[17] U.I. Safronova et al., *J. Phys. B* **44** 035005 (2011).

[18] U.I. Safronova, A.S. Safronova and P. Beiersdorfer, Phys. Rev. A **86** 042510 (2012).

[19] A.E. Kramida and T. Shirai, *Atomic Data and Nuclear Data Tables* **95** 305 (2009).

[20] A. Kramida, *Can. J. Phys.* **89** 551 (2011).

[21] S. Aggarwal, A.K.S. Jha and M. Mohan, *Can. J. Phys.* **91** 394 (2013).

[22] S. Aggarwal, M. Mohan and N. Singh, *Can. J. Phys.* **92** 177 (2014).

[23] A. Kramida and T. Shirai, *J. Phys. Chem. Ref. Data* **35** 423 (2006).

[24] J.O. Ekberg, R. Kling and W. Mende, *Phys. Scr.* **61** 146 (2000).

[25] L. Iglesias, V. Kaufman, O. Garcia-Riquelme and, F.R. Rico, *Phys. Scr.* **31** 173 (1985).

[26] J. Sugar and V. Kaufman, *Phys. Rev. A* **12** 994 (1975).

[27] U.I. Safronova and A.S. Safrnova, *J. Phys. B* **43** 074026 (2010).

[28] Dipti, T. Das, L. Sharma and R. Srivastava, *Phys. Scr.* **86** 035301 (2012).

[29] Y. Padpaly, J.E. Rice, P. Beiersdorfer, M.L. Reinke, J. Clementson and H.S. Barnard, *Can. J. Phys.* **89** 591 (2011).

[30] C.P. Ballance, S.D. Loch, M.S. Pindzola and D.C. Griffin, *J. Phys. B* **46** 055202 (2013).

[31] M.L. Qiu, R.F. Zhao, X.L. Guo, Z.Z. Zhao, X.W. Li, S.Y. Du, J. Xiao, K. Yao, C.Y. Chen, R. Hutton and Y. Zou, *J. Phys. B* **47** 175002 (2014).

[32] W. Jun, Z. Hong and Cheng Xin-Lu, *Chin. Phys. B* **22** 085201 (2013).

[33] J. Clementson, P. Beiersdorfer, T. Brage and M.F. Gu, *Atomic Data and Nuclear Data Tables* **100** 577 (2014).

[34] V. Jonauskas, G. Gaigalas and S.C. Kü, *Atomic Data and Nuclear Data Tables* **98** 19(2012).

[35] P. Bogdanovich and R. Kisielius, *Atomic Data and Nuclear Data Tables* **98** 557 (2012).

[36] P. Bogdanovich and R. Kisielius, *Atomic Data and Nuclear Data Tables* **99** 580 (2013).

[37] S. Aggarwal, *Chin. Phys. B* **23** 093203 (2014).

[38] A. Zigler, H. Zmora, N. Spector, M. Klapisch, J.L. Schwob and A. Bar-Shalom, *J. Opt. Sco. Am.* **70** 129 (1980).

[39] P. Mandelbaum, M. Klapisch and A. Bar-Shalom et al., *Phys. Scr.* **27** 39 (1983).

[40] N. Tragin, J.P. Geindre, P. Monier, J.C. Gauthier, C. Chenais-Popovics, J.F. Wyart and C. Bauche-Arnoult, *Phys. Scr.* **37** 72 (1988).

[41] R. Neu and K.B. Fournier, Ögl Schl and J. Rice, *J. Phys. At. Mol. Opt. Phys.* **30** 5057 (1997).

[42] R.C. Isler, R.V. Neidigh and R.D. Cowan, *Phys. Lett. A* **63** 295 (1977).

[43] E. Hinnov and M. Mattioli, *Phys. Lett. A* **66** 109 (1978).

[44] M. Finkenthal et al., *Phys. Lett. A* **127** 255 (1988).

[45] J. Sugar, V. Kaufman and W.L. Rowan, *J. Opt. Sco. Am. B* **10** 799 (1993).

[46] K. Asmussen et al., *Nucl. Fusion* **38** 967 (1998).

[47] R. Neu et al., *Nucl. Fusion* **45** 209 (2005).

[48] C. Biedermann, R. Radtke, R. Seidel and T. Pütterich, *Phys. Scr.* **T134** 014026 (2009).

[49] R. Causey, K. Wilson, T. Venhaus and W.R. Wampler, *J. Nucl. Mater.* **266-299** 467(1999).

[50] B. Lipschultz et al., MIT Plasma Science and Fusion Center **RR-10-4** (2010).

[51] A. Pospieszczyk, *Nuclear Fusion Research*, Berlin: Springer, (2006).

[52] G.F. Matthews et al., *Phys. Scr.* **T128** 137 (2007).

[53] T. Lennartsson, H. Nilsson, R. Blackwell-Whitehead, L. Engstrom and S. Huldt, *J. Phys. B* **44** 245001 (2011).

[54] C.H. Skinner, *Can. J. Phys.* **T134** 014022 (2009)

[55] R.J. Hawryluk et al., *Nucl. Fusion* **49** 065012 (2009).

[56] C.H. Skinner, *Can. J. Phys.* **86** 285 (2008).

[57] S.E. Yoca, P. Quinet, P. Palmeri and E. Biemont, *J. Phys. B* **45** 065001 (2012).

[58] P. Jönsson, A. Alkauskas and G. Gaigalas, *Atomic Data and Nuclear Data Tables* **99** 431 (2013).

[59] K.T. Cheng, Y.K. Kim and J.P. Desclaux, *Atomic Data and Nuclear Data Tables* **24** 111 (1979).

[60] E.P. Ivanova and A.V. Glushkov, *J. Quant. Spectrosc. Radiat. Transfer* **36** 127 (1986).

[61] D.H. Sampson, H.L. Zhang and J.C. Fontes, *At. Data Nuc. Data Tables* **48** 25–90 (1991).

[62] S. Suckewer and E. Hinnov, *Phys. Rev. Lett.* **41** 756 (1978).

[63] J.J. Chang, *Phys. Rev. A* **3** 791 (1975).

[64] J.J. Chang, *J. Phys. B* **8** 2327 (1975).

[65] J.J. Chang, *J. Phys. B* **10** 3195 (1977).

[66] P.G. Burke, A. Hibbert and W.D. Robb, *J. Phys. B* **4** 153 (1971).

[67] N.S. Scott and P.G. Burke, *J. Phys. B* **13** 4299 (1980).

[68] N.S. Scott and K.T. Taylor, *Comput. Phys. Commun.* **25** 347 (1982).

[69] P.H. Norrington (2009), `http://www.am.qub.ac.uk/DARC/`

[70] I.P. Grant, B.J. McKenzi, P.H. Norrington, D.F. Mayers and N.C. Pyper, *Comput. Phys. Commun.* **21** 207 (1980).

[71] S. Aggarwal, J. Singh and M. Mohan, *Chin. Phys. B* **22** 033201 (2013).

[72] P. Quinet, *J. Phys. B* **45** 025003 (2012).

[73] A.K. Singh, S. Aggarwal and M. Mohan, *Phys. Scr.* **88** 035301 (2013).

[74] S. Aggarwal, J. Singh and M. Mohan, *Atomic Data and Nuclear Data Tables* **99** 704 (2013).

[75] A. Goyal, I. Khatri, S. Aggarwal, A.K. Singh and M. Mohan, *Can. J. Phys.* (article in press)

[76] R. Szmytkowski and J. Hinze, *J. Phys. B* **29** 761 (1996).

[77] P.J.A. Buttle, *J. Rev. A* **160** 719 (1967).

[78] P. Beiersdorfer, J.K. Lepson, M.B. Schneider and M.P. Bode, *Phys. Rev. A* **86** 012509 (2012).

[79] M.F. Gu, *Can. J. Phys.* **86** 675 (2011).

[80] P.G. Burke, K.A. Berrington and C.V. Sukumar, *J. Phys. B* **14** 289 (1981).

[81] `http://physics.nist.gov/cgi-bin/ASD/energy1.pl`